PHYSICAL REVIEW E **68**, 030101(R) (2003)

Persistent global power fluctuations near a dynamic transition in electroconvection

Tibor Tóth-Katona,[1,*] John R. Cressman,[2] Walter I. Goldburg,[2] and James T. Gleeson[1]
[1]*Department of Physics, Kent State University, P.O.B. 5190, Kent, Ohio 44242, USA*
[2]*Department of Physics and Astronomy, University of Pittsburgh, Pittsburgh, Pennsylvania 15260, USA*
(Received 25 November 2002; published 10 September 2003)

This is a study of the global fluctuations in power injection and light transmission through a liquid crystal just above the onset of electroconvection. The source of the fluctuations is identified as the creation and annihilation of defects. They are spatially uncorrelated and yet temporally correlated. The temporal correlation is seen to persist for extremely long times. There seems to be an especially close relation between defect creation or annihilation in electroconvection and thermal plumes in Rayleigh-Bénard convection.

DOI: 10.1103/PhysRevE.68.030101 PACS number(s): 05.40.−a, 61.30.−v, 47.65.+a, 47.52.+j

Recently, the nature of fluctuations of global quantities such as power injection or dissipation in systems held far from equilibrium has become of intense interest [1,2]. Such spatiotemporal fluctuations in physical quantities are often as important as their mean values. This is especially true for systems that are far from the equilibrium. Examples include violent storms, stock market swings, sun spots, volcanic activities, and floods. In this work, we concentrate on global fluctuations in a driven system that is held out of equilibrium by the continuous injection of energy. This energy is ultimately dissipated as heat, and the mean system properties, e.g., its temperature, remain constant in time.

It is useful to recall the case in equilibrium systems with macroscopic size, where the standard deviation σ_X of a global variable X, such as energy or entropy, is such that $\sigma_X/X \sim \sqrt{1/N}$ where N represents the system size, because many statistically independent fluctuations are present. Even near a second order phase transition the fluctuations will average out if the sample size is larger than the thermal correlation length. Near thermal equilibrium, the fluctuation dissipation theorem (FDT) relates σ_X to the system's susceptibility to changes in the intensive variable complementary to X. For strongly driven systems one cannot make such general statements about fluctuations in global quantities. The FDT does not apply, and there is no guarantee that $\sigma_X \ll X$. However, when such a system is driven only slightly above its first bifurcation point, only a small number of spatially and temporally coherent modes will be excited and therefore σ_X/X can be large. Thus, one may begin to understand the origin and scaling of the fluctuations in driven, nonequilibrium systems.

We discuss here a robust model system for studying nonequilibrium behavior: electroconvection (EC) in liquid crystals. We identify the modes responsible for the fluctuations in power injection P as defects (dislocations) in the convection roll pattern. Since such a system can momentarily store energy, the fluctuations in injected and dissipated power need not be the same. This system permits straightforward, simultaneous, and temporally resolved measurement of both localized spatial structures and global characteristics. The principal bifurcation in EC occurs above a critical driving voltage U_c, i.e., at the onset $\varepsilon \equiv (U/U_c)^2 - 1 = 0$ where convecting rolls appear. A small increase in U above U_c generates dislocations (defects) that translate across the plane of the liquid crystal (LC) and have a finite lifetime (see Fig. 1) leading to a state often called defect turbulence [3]. We have found that defects are spatially uncorrelated. Nevertheless, temporal correlations in P are persistent, indicating an underlying order to this chaotic system and permitting the definition of a sharply defined frequency f^*.

The experiments were performed on planarly oriented (nematic director parallel to the bounding glass plates) LC samples of methoxy benzylidene-butyl aniline (MBBA), Phase V (P5) [4] and Mischung 5 (M5) [5]. All samples were prepared with appropriate electrical conductivities and the measurements were made under temperature-controlled conditions. The active area A of the samples was varied between $A \approx 0.01$ cm^2 and 1 cm^2 while their thickness d ranged between 16.6 ± 0.2 μm and 52 ± 1 μm, providing aspect ratios $s = \sqrt{A}/d$ from 36 to 602. All the measurements presented here have been performed at working frequency $f = 100$ Hz which is in terms of relative frequency $f_c/f \sim 5$ for all M5 samples discussed (f_c is the cutoff frequency—see, e.g., Ref. [6]). The details of the experimental setup for the electric power fluctuation measurements have been presented elsewhere [7,8]. We record both $P(t)$ and the optical patterns, and at the same time monitor the transmitted light intensity $I(t)$ integrated over the entire area of the sample.

Figure 2 is a histogram of the power fluctuations, $P - \langle P \rangle$ versus $(P/\sigma_P)^2$, where $\sigma_P = \sqrt{\langle (P - \langle P \rangle)^2 \rangle}$. The straight lines denote a Gaussian distribution having the same

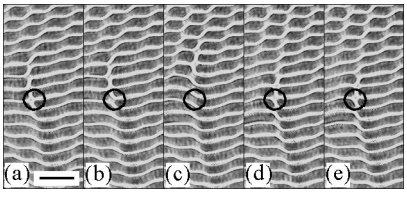

FIG. 1. Snapshots showing the defect creation or annihilation process in time: $t = 0$, 1 s, 15 s, 26 s, and 27 s for (a)–(e), respectively. The circle marks the same location in the cell ($s = 136$, filled with M5, $\varepsilon = 0.2$). The scale bar shows 100 μm.

*On leave from Research Institute for Solid State Physics and Optics, Hungarian Academy of Sciences, P.O.B. 49, H-1525 Budapest, Hungary.
Email address: katona@physics.kent.edu

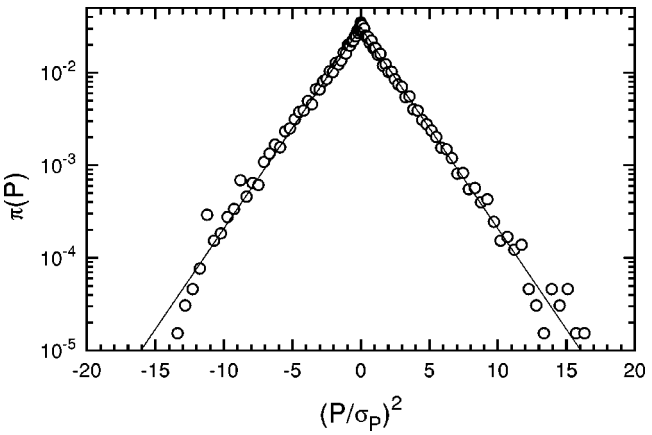

FIG. 2. Probability distribution function of power fluctuations $\pi(P)$ at $\varepsilon=2$ in M5 sample with aspect ratio $s=74$. The solid line represents a Gaussian distribution with no fit parameters.

variance; this is *not* a fit. Figure 3 shows the ε dependence of the normalized variance in power fluctuations, $\sigma_P/\langle P\rangle$ measured in different cells filled with M5 and with various A and d such that s varies by almost a decade. In all cases, as ε is increased above ≈ 0.2, $\sigma_P/\langle P\rangle$ increases dramatically by as much as an order of magnitude. Simultaneous optical observations reveal that the spontaneous creation and annihilation of defects begins at this same value of ε. The stationary EC rolls break up into moving segments; cf. Fig. 1. Measurements in MBBA, not presented here, show that at any given value of ε and d, σ_P increases as $\sqrt{A}$, which is proportional to the number of defects. This strongly suggests that the fluctuations in injected power arises from spatially incoherent sources. This is confirmed by Fig. 2; the central limit theorem predicts the Gaussian distribution for a global measurement having many uncorrelated contributions.

Plotting the data in Fig. 3 in a different way suggests a relation between electroconvection and Rayleigh-Bénard convection (RBC). Observe that the maximum in $\sigma_P/\langle P\rangle$ depends strongly on s. The inset in Fig. 3 is a plot of

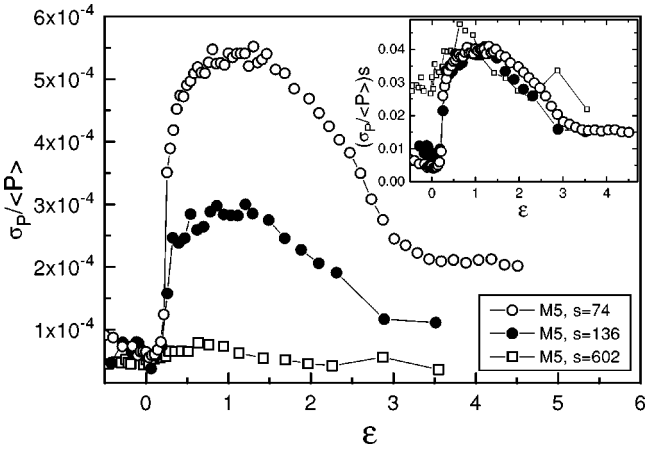

FIG. 3. Dimensionless voltage dependence of the width σ_P of the power fluctuations normalized by the mean value of power $\langle P\rangle$ measured in cells with different aspect ratio s and filled with M5. Inset: $\sigma_P/\langle P\rangle$ normalized with s vs ε.

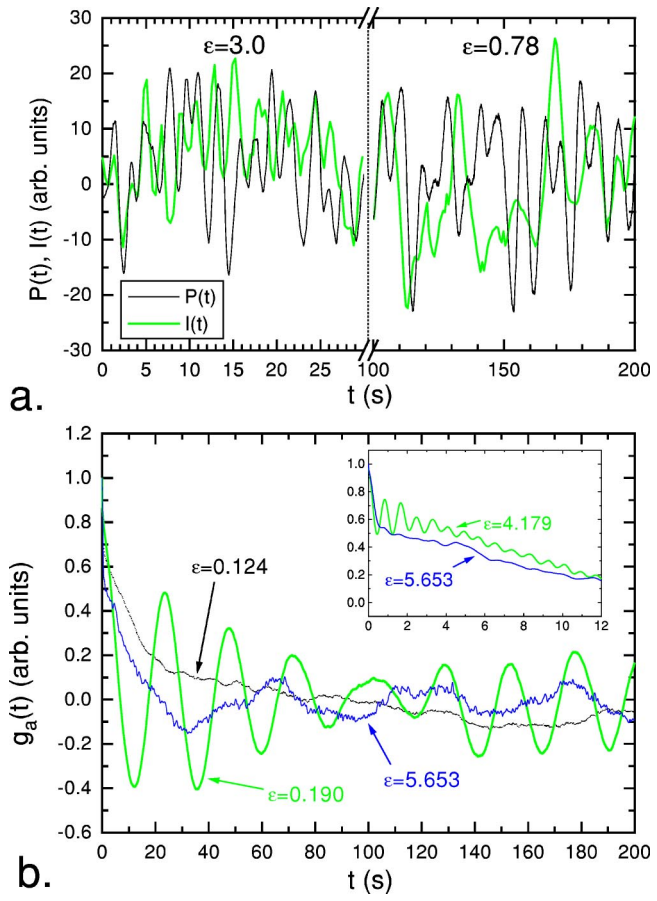

FIG. 4. (Color online) (a) Time series traces of both electric power $P(t)$ and transmitted light intensity $I(t)$ in an MBBA sample for $\varepsilon=3.0$ and $\varepsilon=0.78$ ($A=10$ mm^2, $d=50$ μm). The power and transmitted light intensity were measured at different times. (b) Autocorrelation function $g_a(t)$ measured in an M5 sample ($A=50$ mm^2, $d=52$ μm) for different values of ε. Inset: the same as the main graph for relatively high values of ε where the oscillations in $g_a(t)$ diminish.

$\sigma_P/\langle P\rangle$, scaled by s, as a function of ε. When plotted in this way, all curves collapse for $\varepsilon>0.2$. This affirms that s plays an important role here, as it does for velocity and temperature fluctuations in RBC (see, e.g., Ref. [9]). Similar measurements in MBBA and P5 are found to exhibit the same behavior, suggesting that this is a generic phenomenon in EC. Previous work [10] showed strong dependence of dislocation dynamics on aspect ratio.

Figure 4(a) shows time traces of both $P(t)$ and the integrated transmitted intensity $I(t)$ at $\varepsilon=3.0$ and at $\varepsilon=0.78$. Both of these global measures are quasiperiodic with a dominant frequency f^* that increases with ε. The relative phase between the signals is arbitrary. Note that low-frequency quasiperiodic oscillations in $I(t)$ were also detected in Refs. [11,12] both in local and in global measurements.

The characteristic frequency f^* is also seen in the normalized autocorrelation function $g_a(t)=\langle P(t')P(t'+t)\rangle/\langle P\rangle^2-1$ (average is over t') which is displayed in Fig. 4(b). These measurements were made in an M5 sample ($A=50$ mm^2, $d=52$ μm) for different values of ε. At

$\varepsilon = 0.124$, where EC rolls are well developed but there is no defect creation or annihilation, $g_a(t)$ does not oscillate but decays within 60 s. When the ''varicose'' [13] pattern develops in M5 at $\varepsilon \approx 0.2$ the motion of the rolls starts with infrequent generation/annihilation of defects, and $g_a(t)$ exhibits slow oscillations at frequency f^*. With further increase of ε, f^* increases until $\varepsilon \approx 5$. Above $\varepsilon \approx 5$ the oscillations vanish as their amplitude disappears into the noise and the state of rapid creation and annihilation of defects called dynamic scattering mode 1 (DSM1) [12] takes place [14].

In the range of ε for which oscillations in $g_a(t)$ are seen, they appear to be truly persistent. That is, even for measurement times of many hours, the oscillations persist for the length of the run [$O(10^4)$ oscillation periods]. These measurements were at a value of ε where the sample contained hundreds of defects. It is truly striking that such a large number of spatially uncorrelated defects gives rise to oscillations in $g_a(t)$ correlated over such long times.

Figure 1 displays a series of photographs made at the indicated times t in the liquid crystal M5. The sample thickness is $d = 52$ μm. In this relatively thick sample the varicose pattern persists down to $\varepsilon = 0.2$. At this low level of excitation, the number of dislocations is relatively small and the roll motion is slow. At $t = 0$ we begin watching a single defect of interest (marked with a black circle) as it starts to annihilate [Fig. 1(a)]; 1 s later the annihilation process is finished [Fig. 1(b)] and a defect is created at the same location about 26 s later [Figs. 1(d) and 1(e)]. Note, there is a slight difference in the position of the defects in Figs. 1(a) and 1(e) due to the slow climb motion [15].

The inset of Fig. 5 shows how f^*, obtained from $g_a(t)$, depends on ε for three different aspect ratios. Plotted on the same graph is the inverse of the dislocation lifetimes, as determined by visual inspection, as seen in Fig. 1. Stunningly, the inverse lifetimes, using no adjusted parameters, are within about 5%, of f^*. We submit that this close agreement leaves little doubt that dislocations are the localized excitations responsible for fluctuations in the global injected power. The inset of Fig. 5 also shows that the oscillations in $g_a(t)$ start at $\varepsilon \approx 0.2$—well above the onset of EC.

Optically tracking dislocations is problematic because their number increases and their lifetime decreases with increasing ε. The frame grabber has limited time resolution, and when they are too close together it becomes difficult to track individual dislocations. Measuring power fluctuations has no such limitation. Thus, having identified $1/f^*$ as the defect lifetimes, we are able to determine this quantity beyond the range where it is possible to do so optically. In Fig. 5, f^* is measured over the whole range of ε where defect turbulence [13] occurs.

In EC the continuous generation or annihilation of dislocations (defect turbulence) is predicted to result from an advection of the roll pattern by the large scale, mean flow, which amplifies small undulations in the director field [16]. Because the boundary conditions counteract the bending of rolls, the stress is released by straightening the rolls and topological defects are left behind. A number of experimental studies have been devoted to the motion of dislocations and the process of their creation and annihilation [13,15,17].

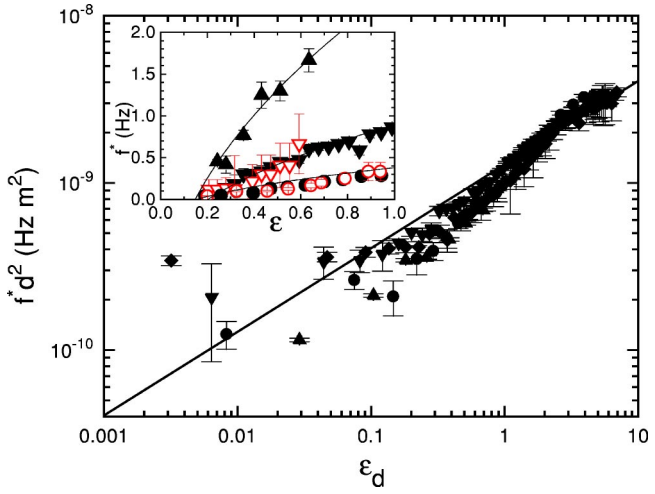

FIG. 5. (Color online) Oscillation frequency f^* as extracted from $g_a(t)$ scaled with the sample thickness (see discussion) as a function of dimensionless voltage ε_d in M5 samples for four different aspect ratios s: 68 [$d = 33.5 \pm 0.6$ μm, down triangles], 74 [$d = 33.4 \pm 0.2$ μm, diamonds], 136 [$d = 52 \pm 1$ μm, circles], and 602 [$d = 16.6 \pm 0.2$ μm, up triangles). The solid line has slope 1/2. Inset: frequency f^* of oscillations extracted from $g_a(t)$ (filled symbols) and determined from the optical observation of the defect creation or annihilation rate (open symbols) as a function of driving voltage ε (shapes of the symbols are the same as in the main figure). Each data point represents the lifetime averaged over ten dislocations.

Most of those measurements were made at relatively low ε, where few dislocations are created. In the context of the present work, the most important result of those studies is that two kinds of forces determine the motion of the defects: a large scale pattern-selection force and a short-range interaction force.

The roles played by dislocations in EC and plumes in RBC appear to be substantially similar. RBC plumes exhibit coherent oscillations with a characteristic frequency [18], and they interact with each other via large scale circulation flow. Most strikingly, the time scales for these two excitations obey the same scaling relations. In RBC, the product of the oscillation frequency and the plate separation collapse, and are proportional to $\sqrt{\mathrm{Ra}}$ where Ra is the Rayleigh number [19]. Figure 5 is a log-log plot of f^* obtained from electric power fluctuation measurements in EC scaled with d^2. The abscissa is $\varepsilon_d = \varepsilon - \text{const}$, where $\varepsilon_d = 0$ is defined as the threshold of the defect creation or annihilation (const ≈ 0.2). The solid line has slope 1/2. All data for different d (and s) collapse on the same line. For the case of RBC, there is a model predicting this behavior [20], but it is not yet clear whether a similar mechanism applies to EC. One should also mention that the theory of defect nucleation, dynamics, and interaction in EC [21] based on the amplitude equation predicts an $\sqrt{\varepsilon}$ dependence. Therefore, our experiments give a clear evidence in the favor of this theory against Ref. [15] based on the presence of gauge field that predicts no ε dependence of the defect motion. Reference [21] also predicts an aspect ratio dependence of the defect velocity (as seen in our measurements and in Ref. [10]) while Ref. [15] does not.

In conclusion, the standard deviation of the fluctuations of the global injected power has been identified as originating with the onset of the spontaneous generation and annihilation of dislocations in the roll pattern. The magnitude of these fluctuations is readily measurable. Furthermore, these fluctuations exhibit persistent temporal correlations, even in the absence of spatial coherence; there is a surprising degree of temporal order embedded in the state called ''defect chaos.'' The scaling properties of the time scale of this correlation are strikingly similar to those observed during the generation of thermal plumes in Rayleigh-Bénard convection. Lastly, this type of observation, particularly the connection between spatially localized and global measurements, is shown to be a powerful and useful technique for studying the increasingly important field of fluctuations in nonequilibrium systems.

We would like to thank Professor V. Steinberg for valuable comments. This work was supported by the National Science Foundation under Grant Nos. DMR-9988614 and DMR-0201805.

[1] D.J. Evans *et al.*, Phys. Rev. Lett. **71**, 2401 (1993); R. Labbé *et al.*, J. Phys. II **6**, 1099 (1996); S.T. Bramwell *et al.*, Nature (London) **396**, 552 (1998); S. Ashkenazi and V. Steinberg, Phys. Rev. Lett. **83**, 3641 (1999); *ibid.* **83**, 4760 (1999); S.T. Bramwell *et al.*, *ibid.* **84**, 3744 (2000); S. Aumaitre *et al.*, Eur. Phys. J. B **19**, 449 (2001); S.T. Bramwell *et al.*, Europhys. Lett. **57**, 310 (2002); G.M. Wang *et al.*, Phys. Rev. Lett. **89**, 050601 (2002).

[2] G. Gallavotti and E.G.D. Cohen, Phys. Rev. Lett. **74**, 2694 (1995); G. Gallavotti, Chaos **8**, 384 (1998).

[3] P. Coullet, L. Gil, and J. Lega, Phys. Rev. Lett. **62**, 1619 (1989); S. Kai and W. Zimmermann, Prog. Theor. Phys. Suppl. **99**, 458 (1989).

[4] Product of Merck Co.

[5] J. Shi, C. Wang, V. Surendranath, K. Kang, and J.T. Gleeson, Liq. Cryst. **29**, 877 (2002).

[6] L. Kramer and W. Pesch, in *Pattern Formation in Liquid Crystals*, edited by Á. Buka and L. Kramer (Springer, New York, 1996), p. 221.

[7] J.T. Gleeson, Phys. Rev. E **63**, 026306 (2001); J.T. Gleeson, N. Gheorghiu, and E. Plaut, Eur. Phys. J. B **26**, 515 (2002).

[8] W.I. Goldburg, Y.Y. Goldschmidt, and H. Kellay, Phys. Rev. Lett. **87**, 245502 (2001).

[9] X.-L. Qiu, and P. Tong, Phys. Rev. E **64**, 036304 (2001).

[10] S. Kai, M. Kohno, M. Andoh, and M. Imasaki, Mol. Cryst. Liq. Cryst. **198**, 247 (1991).

[11] S. Kai and K. Hirakawa, Prog. Theor. Phys. Suppl. **64**, 212 (1978).

[12] S. Kai, M. Araoka, H. Yamazaki, and K. Hirakawa, J. Phys. Soc. Jpn. **46**, 393 (1979).

[13] S. Nasuno, O. Sasaki, S. Kai, and W. Zimmermann, Phys. Rev. A **46**, 4954 (1992).

[14] For the experiments reported here, the DSM1-DSM2 transition was observed at a substantially larger value of ε. This transition point depends on experimental conditions like *f*, *d*, etc.

[15] G. Goren, I. Procaccia, S. Rasenat, and V. Steinberg, Phys. Rev. Lett. **63**, 1237 (1989).

[16] M. Kaiser and W. Pesch, Phys. Rev. E **48**, 4510 (1993).

[17] S. Nasuno, S. Takeuchi, and Y. Sawada, Phys. Rev. A **40**, 3457 (1989); S. Kai, N. Chizumi, and M. Kohno, *ibid.* **40**, 6554 (1989); S. Rasenat, V. Steinberg, and I. Rehberg, *ibid.* **42**, 5998 (1990); S. Rasenat, E. Braun, and V. Steinberg, *ibid.* **43**, 5728 (1991).

[18] X.-L. Qiu, S.H. Yao, and P. Tong, Phys. Rev. E **61**, R6075 (2000); X.-L. Qiu, and P. Tong, Phys. Rev. Lett. **87**, 094501 (2001); Phys. Rev. E **66**, 026308 (2002).

[19] For electroconvection, the control parameter ε should be compared with reduced Rayleigh number, $r \equiv Ra/Ra_t - 1$, in RBC. Here, Ra_t is the threshold for RBC. Plumes are seen for $r \gg 1$.

[20] E. Villermaux, Phys. Rev. Lett. **75**, 4618 (1995).

[21] E. Bodenschatz, W. Pesch, and L. Kramer, Physica D **32**, 135 (1988); E. Bodenschatz, W. Zimmermann, and L. Kramer, J. Phys. (France) **49**, 1875 (1988).